Bernhard Fischer (Autor)

Loss Analysis of Crystalline Silicon Solar Cells using Photoconductance and Quantum Efficiency Measurements

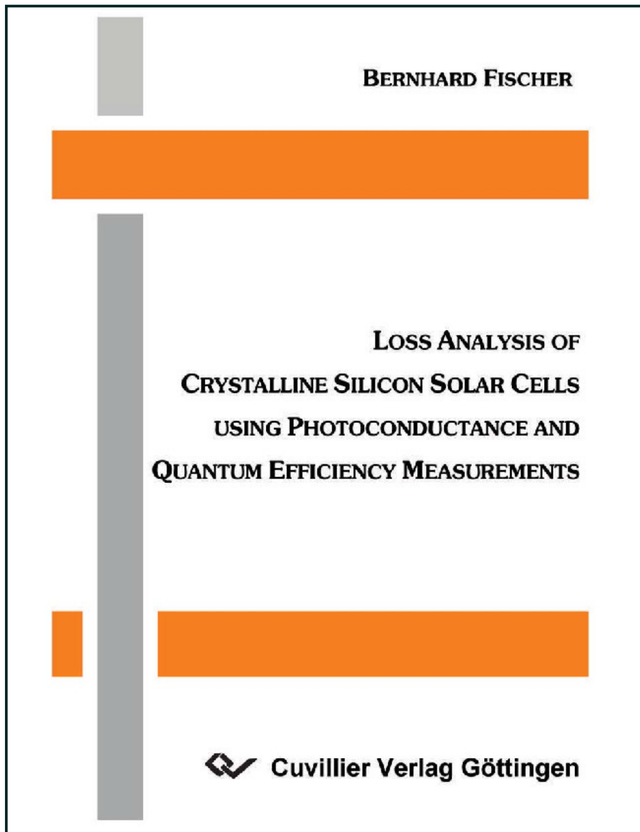

https://cuvillier.de/de/shop/publications/3186

Copyright:
Cuvillier Verlag, Inhaberin Annette Jentzsch-Cuvillier, Nonnenstieg 8, 37075 Göttingen, Germany
Telefon: +49 (0)551 54724-0, E-Mail: info@cuvillier.de, Website: https://cuvillier.de

1 INTRODUCTION

Solar cells are devices to convert sunlight directly into electric energy. A semiconductor can absorb photons with energy larger than the band gap by creation of electron-hole pairs (ehps). These can be separated and led to opposing terminals where they are extracted to perform work in an external circuit. Photon energy in excess of the band gap energy is rapidly lost by the relaxation of the '*hot*' charge carriers to the band edges, which is one major loss mechanism. Photons with energy little below the bandgap can also create ehps if simultaneous absorption of phonons supplies the missing energy. The light absorption probability in this case is only weak, and vanishes quickly if more than one phonon is required. A large fraction of the sun's photons remains unused.

The density of ehps in an illuminated semiconductor without contacts would rise to infinite levels if no further loss mechanisms were present: thermodynamics demands that if photons can be absorbed to create ehps then the reverse process, the radiative recombination of ehps, must occur at the same rate at equilibrium. These are the most fundamental loss mechanisms in photovoltaic cells. They restrict the maximum conversion efficiency under non-concentrated sunlight to approximately 30 % for a semiconductor with the optimum bandgap of 1.1 eV.[1]

The semiconductor treated in this thesis is silicon. It has an indirect bandgap of 1.12 eV and needs phonons to be involved in photon absorption to provide the momentum required for an indirect transition. No phonons are needed to absorb photons with energy above 3.6 eV, the first direct bandgap in silicon, but only few such photons are in the solar spectrum. Thus light absorption is weak compared to a direct bandgap semiconductor such as GaAs, and thick layers, typically 300 microns, are required for sufficient light absorption. Recombination is potentially low by the same argument. Carrier lifetimes in the millisecond range are possible and allow carriers to travel several millimetres before recombining.

'*Loss analysis*' is used in this work for losses that are avoidable in principle. They can be divided into three categories:

- optical losses
- recombination losses
- resistive losses

The analysis of completed solar cells offers only limited insight since too many effects are at work simultaneously. Therefore, it is helpful to examine the physical mechanisms separately using suitable test structures and measurement techniques. Some losses are difficult to assess directly and are preferably calculated using appropriate models or simulation programs. Once the material and device parameters are determined, their consistence can be verified by comparing device simulations with experimental results.

Material inhomogeneity, injection dependence of device parameters and multi-dimensional features of solar cells make the interpretation of measurements difficult. Rather than using multi-dimensional finite element device simulators to take into account all possible interactions and physical effects, this work endeavours to find appropriate one-dimensional representations for the following reasons:

- Having a simple one-dimensional description allows not only to simulate the solar cell characteristics from a set of input parameters but also allows to deduce the input parameters from measurements.
- Device simulations usually yield current-voltage characteristics or quantum efficiency spectra from which the individual losses not revealed. Only after variation of the input parameters does the importance of individual effects become obvious.

Chapter 2 begins with reviewing the foundations of the one-dimensional carrier transport in solar cells and introducing the concepts that will be used throughout this work. It then explains the one-dimensional reduction of more complex problems with two examples: the transport in solar cells with local rear contacts and the lifetime inhomogeneities in multi-crystalline silicon and its effects on solar cell performance and characterisation.

Chapters 3 and 4 describe the applied measurement and evaluation techniques. Quantum efficiency measurements of solar cells provide valuable information about electrical device parameters, loss currents and optical properties. The quasi-steady state photoconductance technique (QSSPC) has proven to be an ideal tool to quantify recombination parameters on test structures. New contributions to both techniques will be described.

The fabrication and analysis of a simple high efficiency solar cell design (RP-PERC, random-pyramid textured passivated emitter and rear solar cell) on monocrystalline silicon is treated in Chapter 5. It focuses on reasons for poor rear surface passivation and material degradation during processing.

Chapter 6 describes the investigations on multicrystalline silicon solar cells, starting with an analysis of state-of-the-art industrial solar cells. Screen printed contacts and the aluminium back surface fields are considered in detail. Finally a high efficiency concept for multicrystalline solar cells is examined that allows high optical current generation by mechanical grooving of the surface and encapsulation in glass.

2 RECOMBINATION AND TRANSPORT IN SOLAR CELLS

2.1 RECOMBINATION

2.1.1 SRH-Recombination

Point-like imperfections in the semiconductor disturb the periodicity of the crystal lattice and therefore create characteristic energy levels E_t within the bandgap. They can capture and release free carriers, both electrons and holes, and therefore assume several charge states. If the Fermi level lies at E_t then two neighbouring charge states are equally probable. Such defects are preferred sites for the recombination of excess carriers in non-equilibrium. Evaluation of the net rates of charge carrier capture and emission at a recombination centre that can assume only two charge states leads to the so-called Shockley-Read-Hall (SRH) recombination lifetime[2]

$$\tau_{SRH} = \tau_p \frac{n_0 + n_1 + \Delta n}{n_0 + p_0 + \Delta n} + \tau_n \frac{p_0 + p_1 + \Delta n}{n_0 + p_0 + \Delta n} . \tag{2-1}$$

It is the parameter that relates the recombination rate R to the excess carrier concentration Δn through $R = \Delta n/\tau_{SRH}$. n_0 and p_0 are the equilibrium electron and hole concentrations and n_1, p_1 the concentrations when the Fermi level coincides with E_t.[i] Equal concentrations of excess electrons and holes is assumed to conserve charge neutrality.[ii] The capture time constants for electrons, $\tau_n = N_t v_{th} \sigma_n$, and holes, $\tau_p = N_t v_{th} \sigma_p$, are proportional to the defect density N_t and the thermal velocity v_{th} of the carriers ($v_{th} \approx 10^7$ cm/s). The proportionality constants are the capture cross sections (ccs) σ_n and σ_p.

Deep levels with energies close to midgap are more detrimental recombination centres than shallow levels near the band edges. Whether the defect state is a donor (charge states $0 \leftrightarrow +$) or an acceptor ($0 \leftrightarrow -$) does not directly enter the formulation, but the capture cross sections in the ionised state are typically larger than in the neutral state because of the coulomb attraction.

The SRH lifetime depends on Δn, also referred to as *injection dependence*. Both in low level injection (*lli*, $\Delta n \ll$ doping) and high level injection (*hli*, $\Delta n \gg$ doping) the SRH-lifetime becomes approaches a constant value, in *hli* generally $\tau_{SRH,hli} \approx \tau_n + \tau_p$. Capture of minority carriers dominates for deep level defects in *lli*, so that $\tau_{SRH,lli} \approx \tau_n$. But the SRH-lifetime does not necessar-

---

[i] i.e. $n_1 = n_i \exp(\beta E_t - \beta E_i) = n_i^2/p_1$ with $\beta = 1/k_B T$ and the intrinsic carrier concentration n_i (10^{10} cm^{-3} at 300 K).[3] The intrinsic Fermi-energy E_i for which $n_0 = p_0 = n_i$, lies slightly above mid-gap because of the difference in the effective densities of states in the valence band, N_V, and conduction band, N_C: $2\,E_i = E_C + E_V + k_B T \ln(N_V/N_C)$.

[ii] The assumption $\Delta n = \Delta p$ breaks down if trapping centres are present (see Section 4.4.1).

ily increase with Δn. If the doping concentration in *p*-type silicon is equal to $n_1 + p_1\, \tau_n/\tau_p$ then τ_{SRH} becomes independent of Δn and will decrease with injection for lower doping concentrations. Figure 2-1 illustrates the injection dependence of a defect for *p*-type Si.

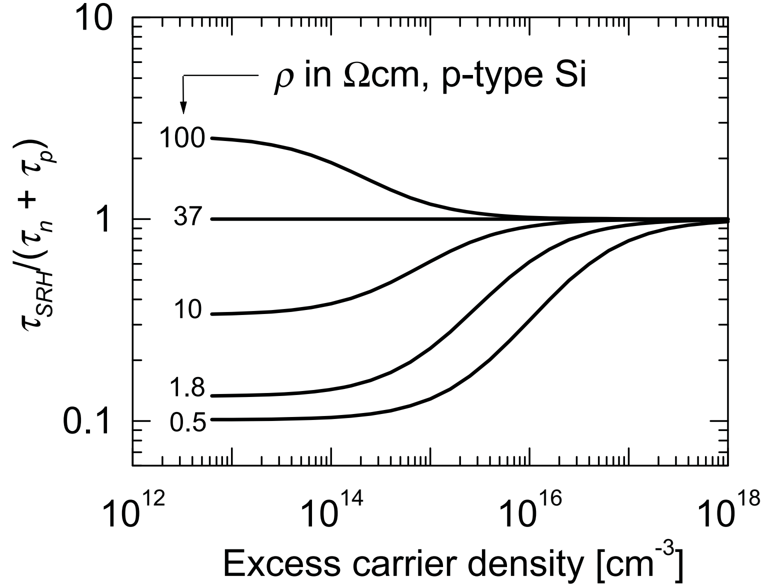

Figure 2-1: *Injection dependence of the recombination lifetime for a single level defect with a ratio of* $\tau_n/\tau_p = 10$ *and an energy level of* $E_t = E_i + 270$ *meV*

If several independent defects are present, their recombination rates add, leading to a carrier lifetime of $\tau_{SRH}^{-1} = \tau_{SRH,1}^{-1} + \tau_{SRH,2}^{-1} + _{...}$. The lifetime for defects that can assume three charge states is given in Appendix A1.

2.1.2 Intrinsic recombination mechanisms

There are two recombination mechanisms in semiconductors that are unavoidable and not technology dependent. *Radiative recombination* is the reverse process of optical absorption and is proportional to the *p-n* product. *Auger recombination* is the reverse process of impact ionisation. It involves a third free charge carrier to which the recombination energy is transferred by exciting it into higher energy levels in its band. From there it relaxes back to the band edge emitting phonons. This third particle will most likely be a majority carrier because of the higher availability. Auger recombination generally dominates over radiative recombination in silicon. It poses an upper limit to the volume lifetime for a given doping and injection level and finally limits the maximum conversion efficiency of silicon solar cells to about 29 %.[4]

Traditionally, the *lli* recombination rate for this three-particle process is written as $R = C_n\, n\, p^2$ in *p*-type and $R = C_p n^2 p$ in *n*-type material.[5] In high injection with $n \approx p \approx \Delta n$ the rate becomes[6,7] $R = C_{hli}\, \Delta n^3$ with the ambipolar Auger coefficient $C_{hli} = C_n + C_p$. The corresponding Auger lifetime is $1/\tau_{Auger} = C_{hli}\, \Delta n^2$. Experimentally, a lower than quadratic dependence, rather $\tau_{Auger} \propto \Delta n^{1.65}$ is observed.[6,8,14] The *lli* relation holds well for very high doping levels but severely underestimates

Auger recombination at lower doping concentrations. Including correlation effects due to the coulomb interaction between electrons and holes enabled Hangleiter and Häcker[9] to resolve the discrepancy, but they restricted their theoretical study to low level injection. A number of empirical parameterisations of the Auger-lifetime in Si for arbitrary injection and doping concentrations appeared over the last years.[10-15] Although the solar cells fabricated in this work are not limited by the Auger process, a reasonably accurate formulation of the Auger-lifetime is important for the determination of emitter saturation currents (see Section 4.5.2) and as a lower limit for volume recombination in the interpretation of lifetime measurements.

The three volume recombination mechanisms are assumed to be independent of each other so that their recombination rates can be added. This results in a volume lifetime of

$$\frac{1}{\tau_{vol}} = \frac{1}{\tau_{SRH}} + \frac{1}{\tau_{Auger}} + \frac{1}{\tau_{rad}} . \qquad (2\text{-}2)$$

2.1.3 Recombination at surfaces

Semiconductor surfaces and also internal surfaces like grain boundaries are a severe disturbance of the crystal lattice periodicity and lead to a continuum of interface states within the band gap. With the interface state density $D_{it}(E)$ (in $\mathrm{cm^{-2}eV^{-1}}$) the SRH formalism must be extended to an integral, which gives the total recombination rate as[16]

$$U = v_{th}\left(np - n_i^2\right)\int_{E_V}^{E_C} \frac{D_{it}}{\sigma_n\left(n+n_1\right)+\sigma_p\left(p+p_1\right)} dE . \qquad (2\text{-}3)$$

The values n_1, p_1 as well as the capture cross sections are now functions of the energy. The carrier densities in eqn. (2-3) refer to their values directly at the surface, which will differ from the bulk values when a surface potential builds up to maintain the charge balance. The formalism of the related band-bending and the definitions for accumulation, depletion and inversion are described in Appendix A2. This recombination rate can be translated into a surface recombination velocity (SRV) S, which relates the total recombination to the excess carrier density in the neutral region adjacent to the surface, $U = \Delta n\, S$. In general, this S is not constant but depends on Δn.

For unpassivated surfaces the effective SRV is practically infinite, sinking all available excess carriers until $\Delta n \approx 0$. The recombination current is then limited by the supply of carriers via diffusion from the bulk. The three possibilities to passivate silicon surfaces are a) to decrease D_{it} by chemically saturating the dangling bonds with e.g. hydrogen or oxygen, b) to repel one carrier type from the surface by means of an electric field (referred to as *field-effect passivation*) and c) the use of highly doped surface layers to suppress one carrier type, referred to as *emitters* or *floating junctions*[17] and *back surface fields*[18] depending on whether the conduction type is changed or not. The most successful rear surface passivation for silicon solar cells consists of a combination. Problems involved with field effect passivation for this purpose will be addressed in Section 5.4.1.